

Average phase factor in the PNJL model

Yuji Sakai,^{1,*} Takahiro Sasaki,^{1,†} Hiroaki Kouno,^{2,‡} and Masanobu Yahiro^{1,§}

¹*Department of Physics, Graduate School of Sciences, Kyushu University, Fukuoka 812-8581, Japan*

²*Department of Physics, Saga University, Saga 840-8502, Japan*

(Dated: November 13, 2018)

The average phase factor $\langle e^{2i\theta} \rangle$ of the QCD determinant is evaluated at finite quark chemical potential (μ_q) with the two-flavor version of the Polyakov-loop extended Nambu–Jona-Lasinio (PNJL) model with the scalar-type eight-quark interaction. For μ_q larger than half the pion mass m_π at vacuum, $\langle e^{2i\theta} \rangle$ is finite only when the Polyakov loop is larger than ~ 0.5 , indicating that lattice QCD is feasible only in the deconfinement phase. A critical endpoint (CEP) lies in the region of $\langle e^{2i\theta} \rangle = 0$. The scalar-type eight-quark interaction makes it shorter a relative distance of the CEP to the boundary of the region. For $\mu_q < m_\pi/2$, the PNJL model with dynamical mesonic fluctuations can reproduce lattice QCD data below the critical temperature.

PACS numbers: 11.30.Rd, 12.40.-y

I. INTRODUCTION

The thermodynamics of quantum chromodynamics (QCD) is well defined, since QCD is renormalizable and parameter free. Nevertheless, the thermodynamics is not understood at lower temperature (T) because of its nonperturbative nature. The thermodynamics is closely related to not only natural phenomena such as compact stars and the early universe but also laboratory experiments such as relativistic heavy-ion collisions. Lattice QCD (LQCD) is a first-principle calculation, but it has the well-known sign problem when the quark-number chemical potential (μ_q) is real; for example, see Ref. [1]. So far, several approaches have been proposed to circumvent the difficulty; for example, the reweighting method [2], the Taylor expansion method [3] and the analytic continuation from imaginary μ_q to real μ_q [4–7]. However, these are still far from perfection particularly at $\mu_q/T \gtrsim 1$.

The success of the approaches is linked to how difficult the sign problem is. As a good index of the difficulty, one can consider the average of the phase factor

$$e^{2i\theta} = \frac{\det(D + \mu_q \gamma_0 + m)}{\det(D + \mu_q \gamma_0 + m)^*} \quad (1)$$

of the Fermion determinant. If the average of the phase factor is much smaller than 1, this means that there are severe cancellations in the path integral of the QCD partition function. In this situation, LQCD simulations are not feasible.

The average is obtained by taking the expectation value of the phase factor in the phase-quenched theory in which the Fermion determinant is replaced by the absolute value. In the two-flavor case, the average is

$$\langle e^{2i\theta} \rangle = \frac{Z_{1+1}}{Z_{1+1*}}, \quad (2)$$

where Z_{1+1} stands for the partition function of the ordinary two-flavor theory and Z_{1+1*} represents that of the two-flavor phase-quenched theory in which one of two flavors is changed into a conjugate flavor. For comparison of the 1+1* system with the 1+1 system, let us introduce the modified isospin chemical potential μ_I related to the isospin chemical potential μ_{iso} as $\mu_I = \mu_{\text{iso}}/2$. When the 1+1 system has a value of μ_q , the 1+1* system possesses the same value of μ_I .

It is not easy to calculate the average phase factor with LQCD even for small μ_q/T . Actually, several LQCD results on the average phase factor are spotted; see Ref. [11] and references therein. It is then important to make a systematic analysis on the phase factor by using effective theories. This was done by the chiral perturbation theory [8, 9]. The result is consistent with LQCD one [11] when T is lower than the critical one T_c . However, the theory is not valid for $T > T_c$.

Recently, the average phase factor at $T > T_c$ was calculated by the random matrix theory [10] and the Nambu–Jona-Lasinio (NJL) model [12]. When the saddle-point approximation is applied to the path integrals in the partition functions Z_{1+1} and Z_{1+1*} , the average phase factor can be described by

$$\langle e^{2i\theta} \rangle \approx \frac{\sqrt{\det H_{1+1*}}}{\sqrt{\det H_{1+1}}} e^{-\beta V(\Omega_{1+1} - \Omega_{1+1*})}, \quad (3)$$

where $\beta = 1/T$, Ω is the thermodynamic potential at mean field level and H is the Hessian matrix showing static fluctuations (SF) at the saddle point. The average phase factor thus obtained is dominated not by the exponential factor $e^{-\beta V(\Omega_{1+1} - \Omega_{1+1*})}$ but by the SF factor $\sqrt{\det H_{1+1*}}/\sqrt{\det H_{1+1}}$ [12], because $\Omega_{1+1} = \Omega_{1+1*}$ in the normal phase with no pion condensate and the SF factor is zero in the pion condensate phase; this will be explained explicitly in subsection II B. Thus, the average phase factor should be calculated with the mean field (MF) approximation plus SF corrections. This framework is referred to as MF+SF in the present paper.

The NJL model describes the chiral phase transition [13–18], but not the deconfinement transition. The Polyakov-loop extended Nambu–Jona-Lasinio (PNJL) model [19–38] was constructed to treat both the transitions simultaneously. Very recently, the PNJL model was shown to be successful

*sakai@phys.kyushu-u.ac.jp

†sasaki@phys.kyushu-u.ac.jp

‡kounoh@cc.saga-u.ac.jp

§yahiro@phys.kyushu-u.ac.jp

in reproducing LQCD data for imaginary quark chemical potential [34, 35], imaginary quark and isospin chemical potentials [36] and real isospin chemical potential [38]. Thus, the PNJL model is one of the most reliable models.

In this paper, we evaluate the average phase factor by the PNJL model in the MF+SF framework and investigate a relation between the Polyakov-loop and the average phase factor. For thermal systems at $\mu_I = \mu_q = 0$ and at $\mu_I > 0$ and $\mu_q = 0$, the scalar-type eight-quark interaction is essential for the PNJL model to reproduce LQCD data [35, 38]. We then analyze an effect of the eight-quark interaction on the average phase factor, too. Finally, we consider dynamical mesonic fluctuations (DF), instead of static mesonic fluctuations, to compare the PNJL results with LQCD data.

This paper is organized as follows. In Sec. II, we recapitulate the PNJL model and a way of calculating the average phase factor. The numerical results are shown in Sec. III. Effects of the Polyakov loop, the eight-quark interaction, static fluctuations and dynamical mesonic fluctuations are investigated. Section IV is devoted to summary.

II. FORMALISM

In this section, we first explain the PNJL model in the MF level for the case of finite μ_q and μ_I and treat SF in order to evaluate the average phase factor.

A. PNJL model

The Lagrangian of the two-flavor PNJL model in Euclidean spacetime is

$$\begin{aligned} \mathcal{L} = & \bar{q}(\gamma_\nu D^\nu - \gamma_4 \hat{\mu} + \hat{m}_0)q + G_s [(\bar{q}q)^2 + (\bar{q}i\gamma_5 \vec{\tau}q)^2] \\ & + G_{s8} [(\bar{q}q)^2 + (\bar{q}i\gamma_5 \vec{\tau}q)^2]^2 - \mathcal{U}(\Phi[A], \Phi[A]^*, T), \end{aligned} \quad (4)$$

where $D^\nu = \partial^\nu + iA^\nu$ and $A^\nu = \delta_0^\nu g A_a^0 \frac{\lambda_a}{2}$ with the gauge field A_a^ν , the Gell-Mann matrix λ_a and the gauge coupling g . The coupling constant G_s (G_{s8}) represents a strength of the scalar-type four-quark (eight-quark) interaction. The Polyakov potential \mathcal{U} of (18) is a function of the Polyakov loop Φ and its Hermitian conjugate Φ^* .

The chemical potential matrix $\hat{\mu}$ is defined by $\hat{\mu} = \text{diag}(\mu_u, \mu_d)$ with the u -quark (d -quark) number chemical potential μ_u (μ_d), while $\hat{m}_0 = \text{diag}(m_0, m_0)$. The chemical potential matrix is described by μ_q and μ_I as

$$\hat{\mu} = \mu_q \tau_0 + \mu_I \tau_3, \quad (5)$$

where τ_0 is the unit matrix and τ_i ($i = 1, 2, 3$) are the Pauli matrices in flavor space. The μ_q and μ_I are related to the baryon and isospin chemical potentials, μ_B and μ_{iso} , coupled respectively to the baryon charge B and to the isospin charge \bar{I}_3 as

$$\mu_q = \frac{\mu_u + \mu_d}{2} = \frac{\mu_B}{3}, \quad \mu_I = \frac{\mu_u - \mu_d}{2} = \frac{\mu_{iso}}{2}. \quad (6)$$

For later convenience, we use μ_I instead of μ_{iso} and call it the isospin chemical potential simply. The 1+1 and the 1+1* theory correspond to taking $(\mu_q, \mu_I) = (\mu_q, 0)$ and $(0, \mu_q)$, respectively, in \mathcal{L} of (4). In the limit of $m_0 = \mu_I = 0$, the PNJL Lagrangian has the $SU_L(2) \times SU_R(2) \times U_V(1) \times SU_C(3)$ symmetry. For $m_0 \neq 0$ and $\mu_I \neq 0$, it is reduced to $U_{I_3}(1) \times U_V(1) \times SU_C(3)$.

The Polyakov-loop operator $\hat{\Phi}$ and its Hermitian conjugate $\hat{\Phi}^\dagger$ are defined as

$$\hat{\Phi} = \frac{1}{3} \text{Tr} L, \quad \hat{\Phi}^* = \frac{1}{3} \text{Tr} L^\dagger, \quad (7)$$

with

$$L(\mathbf{x}) = \mathcal{P} \exp \left[i \int_0^\beta d\tau A_4(\mathbf{x}, \tau) \right], \quad (8)$$

where \mathcal{P} is the path ordering and $A_4 = iA^0$. In the Polyakov gauge, L can be written in a diagonal form in color space [20]:

$$L = e^{i\beta(\phi_3 \lambda_3 + \phi_8 \lambda_8)}. \quad (9)$$

In the MF level, ϕ_3 and ϕ_8 are treated as classical variables [25].

The spontaneous breakings of the chiral and the $U_{I_3}(1)$ symmetry are described, respectively, by the chiral condensate $\sigma = \langle \bar{q}q \rangle$ and the charged pion condensate [28]

$$\pi^\pm = \frac{\pi}{\sqrt{2}} e^{\pm i\alpha} = \langle \bar{q}i\gamma_5 \tau_\pm q \rangle. \quad (10)$$

Since the phase α represents the direction of the $U_{I_3}(1)$ symmetry breaking, we take $\alpha = 0$ for convenience. The pion condensate is then expressed by

$$\pi = \langle \bar{q}i\gamma_5 \tau_1 q \rangle. \quad (11)$$

Making the MF approximation [18, 28], one can obtain the MF Lagrangian as

$$\begin{aligned} \mathcal{L}_{\text{MF}} = & \bar{q}(\gamma_\nu D^\nu - \gamma_4 \hat{\mu} + M \tau_0 + N i\gamma_5 \tau_1)q \\ & + G_s [\sigma^2 + \pi^2] + 3G_{s8} (\sigma^2 + \pi^2)^2 + \mathcal{U} \end{aligned} \quad (12)$$

with

$$\begin{aligned} M &= m_0 - 2[G_s + 2G_{s8}(\sigma^2 + \pi^2)]\sigma, \\ N &= -2[G_s + 2G_{s8}(\sigma^2 + \pi^2)]\pi. \end{aligned} \quad (13)$$

The quark propagator \mathcal{S} in the MF level, that has off-diagonal elements in flavor space, is obtained by

$$\mathcal{S}^{-1}(p) = \begin{pmatrix} \gamma_\nu P^\nu - \mu_u \gamma_4 + M & -i\gamma_5 N \\ i\gamma_5 N & \gamma_\nu P^\nu - \mu_d \gamma_4 + M \end{pmatrix} \quad (14)$$

where $P^\nu = p^\nu - A^\nu$. Performing the path integral in the PNJL partition function

$$Z_{\text{MF}} = \int Dq D\bar{q} \exp \left[- \int d^4x \mathcal{L}_{\text{MF}} \right], \quad (15)$$

we can get the thermodynamic potential (per unit volume),

$$\begin{aligned} \Omega_{\text{MF}} = -T \ln(Z_{\text{MF}})/V = & -2 \sum_{i=\pm} \int \frac{d^3\mathbf{p}}{(2\pi)^3} \left[3E_i(\mathbf{p}) \right. \\ & + \frac{1}{\beta} \ln [1 + 3(\Phi + \Phi^* e^{-\beta E_i^-(\mathbf{p})}) e^{-\beta E_i^-(\mathbf{p})} + e^{-3\beta E_i^-(\mathbf{p})}] \\ & + \frac{1}{\beta} \ln [1 + 3(\Phi^* + \Phi e^{-\beta E_i^+(\mathbf{p})}) e^{-\beta E_i^+(\mathbf{p})} + e^{-3\beta E_i^+(\mathbf{p})}] \left. \right] \\ & + G_s[\sigma^2 + \pi^2] + 3G_{s8}(\sigma^2 + \pi^2)^2 + \mathcal{U} \end{aligned} \quad (16)$$

with

$$E_{\pm}^{\pm}(\mathbf{p}) = E_{\pm}(\mathbf{p}) \pm \mu_q, \quad (17)$$

where $E_{\pm}(\mathbf{p}) = \sqrt{(E(\mathbf{p}) \pm \mu_1)^2 + N^2}$ and $E(\mathbf{p}) = \sqrt{\mathbf{p}^2 + M^2}$. The momentum integral in (16) is regularized by the three-dimensional cutoff Λ .

We use \mathcal{U} of Ref. [25]:

$$\begin{aligned} \mathcal{U} = T^4 \left[-\frac{a(T)}{2} \Phi^* \Phi \right. \\ \left. + b(T) \ln(1 - 6\Phi\Phi^* + 4(\Phi^3 + \Phi^{*3}) - 3(\Phi\Phi^*)^2) \right], \end{aligned} \quad (18)$$

$$a(T) = a_0 + a_1 \left(\frac{T_0}{T}\right) + a_2 \left(\frac{T_0}{T}\right)^2, \quad b(T) = b_3 \left(\frac{T_0}{T}\right)^3. \quad (19)$$

The parameters of \mathcal{U} are adjusted to LQCD data in the heavy-quark (pure-gauge) limit [39, 40]; the resultant parameter set is shown in Table I. In the limit, the Polyakov potential yields a first-order deconfinement phase transition at $T = T_0$. Since the first-order transition takes place at $T = 270$ MeV in LQCD, T_0 is often set to 270 MeV in the PNJL calculation. In the light-quark case, however, the PNJL calculation with this value of T_0 yields a larger value of T_c than the full LQCD prediction $T_c = 173$ MeV [41–43]. Therefore, we rescale T_0 to 200 MeV to reproduce $T_c = 173$ MeV [35].

a_0	a_1	a_2	b_3
3.51	-2.47	15.2	-1.75

TABLE I: Summary of the parameter set in the Polyakov-potential sector determined in Ref. [25]. All parameters are dimensionless.

In the NJL sector, two parameter sets are taken; in the first set G_{s8} is finite, while in the second set it is zero. The first set is $\Lambda = 0.6315$ GeV, $G_s = 4.673$ [GeV⁻²], $G_{s8} = 452.12$ [GeV⁻⁸] and $m_0 = 5.5$ MeV. This set reproduces not only the pion decay constant $f_\pi = 93.3$ MeV and the pion mass $m_\pi = 139$ MeV at vacuum but also LQCD data [41–43] on σ and $|\Phi|$ for thermal systems with no μ_q and μ_1 [35]. The second set is $\Lambda = 0.6315$ GeV, $G_s = 5.498$ GeV⁻², $G_{s8} = 0$ and $m_0 = 5.5$ MeV. This set can reproduce the pion decay constant and the pion mass at vacuum, but not LQCD data for thermal systems with no μ_q and μ_1 . Thus, the first set with finite G_{s8} is more reliable.

B. Average phase factor

As mentioned in section I, we have to consider fluctuations to mean fields to evaluate the average phase factor. In this subsection, we consider static fluctuations (SF).

In the path-integral representation of the partition function Z or the thermodynamic potential Ω , ϕ_3 and ϕ_8 are fundamental fields rather than Φ and Φ^* . This means that we should solve the stationary conditions

$$\frac{\partial \Omega}{\partial \varphi} = 0 \quad (20)$$

for $\varphi = (\sigma, \vec{\pi}, \phi_3, \phi_8)$ rather than $\varphi = (\sigma, \vec{\pi}, \Phi, \Phi^*)$ [25], although the solutions are not so different between the two cases. However, the first case does not guarantee that Ω is real. Following Ref. [25], we then put $\phi_8 = 0$ to keep Ω real. Noting that the first-order derivative with respect to ϕ_8 does not vanish, we expand Ω up to quadratic terms of fluctuations:

$$\Omega = \Omega_{\text{MF}} + \left(\frac{\delta \Omega}{\delta \varphi_i} \right)_{\text{MF}} \delta \varphi_i + \frac{1}{2} \left(\frac{\delta^2 \Omega}{\delta \varphi_i \delta \varphi_j} \right)_{\text{MF}} \delta \varphi_i \delta \varphi_j, \quad (21)$$

where $\varphi = \sum_i \delta \varphi_i + \varphi_{\text{MF}}$ for mean fields φ_{MF} and static (constant) fluctuations $\delta \varphi_i$. Since first-order terms in $\delta \varphi_i$ are purely imaginary, we can regard an integral over $\delta \varphi_i$ as a Fourier integral. We then obtain

$$Z = \int \prod_i d(\delta \varphi_i) \exp \left[-\frac{V}{T} \Omega \right] = \frac{1}{\mathcal{N}} \exp \left[-\frac{V}{T} \tilde{\Omega} \right] \quad (22)$$

with

$$\tilde{\Omega} = \left\{ \Omega_{\text{MF}} + \frac{1}{2} \left(\frac{\delta^2 \Omega}{\delta^2 \phi_8} \right)_{\text{MF}}^{-1} \left(\frac{\delta \Omega}{\delta \phi_8} \right)_{\text{MF}}^2 \right\} \quad (23)$$

and

$$\mathcal{N} = \left(\frac{V}{2\pi T} \right)^{\frac{n}{2}} \|\det H\|^{\frac{1}{2}}, \quad (24)$$

where n is the number of fields and H is the Hessian matrix defined by

$$H = \left[\frac{\delta^2 \Omega}{\delta \varphi_i \delta \varphi_j} \right]_{\text{MF}}. \quad (25)$$

Obviously, the Hessian matrix describes static fluctuations of mean fields φ_{MF} . Therefore, the average phase factor is obtained by (3) with Ω replaced by $\tilde{\Omega}$. The average phase factor thus obtained is a function of the φ_{MF} that satisfy the stationary conditions (20). Thus, the average phase factor is calculable in the MF+SF framework.

The static fluctuations are composed of those of σ and π and of ϕ_3 and ϕ_8 . In subsection III C, we keep treating static fluctuations for ϕ_3 and ϕ_8 , but consider dynamical fluctuations for σ and π , that is, σ and π mesons.

It was revealed in Ref. [12] with the NJL model that in the pion condensate phase, where π_{MF} is finite and then a massless mode appears, the average phase factor vanishes owing

to det $H_{1+1^*} = 0$. Obviously, this is true also for the PNJL model, as shown in (25). In the normal phase with no pion condensate, Ω_{1+1} and Ω_{1+1^*} are the same in the MF level, so that the average phase factor is determined by only the SF factor $\sqrt{\det H_{1+1^*}}/\sqrt{\det H_{1+1}}$.

LQCD calculation in Ref. [6] has a lattice size $16^3 \times 4$. Hence, the three-dimensional volume is $V = (16a)^3$ for a lattice spacing a and the inverse of temperature is $1/T = 4a$. The four-dimensional volume is then obtained by $V/T = 64T^{-4}$. This four-dimensional volume is taken also for the PNJL model in its calculation of the average phase factor.

III. NUMERICAL RESULTS

A. Average phase factor and Polyakov loop

Solving the stationary conditions (20) and inserting the solutions in (3), one can obtain Φ , π and $\langle e^{2i\theta} \rangle$ as a function of T and μ_q . As a shorthand notation, we use Φ for Φ_{1+1} and π for π_{1+1^*} . All the calculations in this subsection are done without the scalar-type eight-quark interaction; roles of the eight-quark interaction will be discussed in subsection III B.

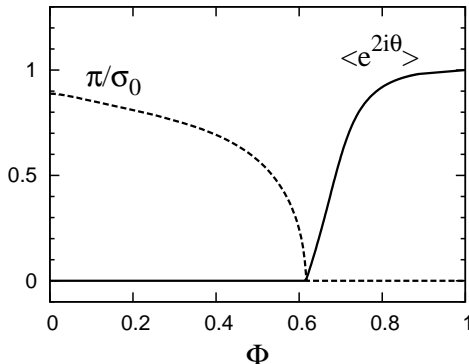


Fig. 1: Φ dependence of the scaled pion condensate π/σ_0 and the average phase factor $\langle e^{2i\theta} \rangle$ at $\mu_q = 100$ MeV. Here, σ_0 is a chiral condensate at $T = \mu_q = 0$. The former is plotted by a dashed curve, while the latter is by a solid curve.

In Fig. 1, we plot $(\Phi(T), \pi(T))$ by a dashed line and $(\Phi(T), \langle e^{2i\theta} \rangle(T))$ by a solid line, varying T with μ_q fixed at 100 MeV. Since Φ is an increasing function of T [35], an increase of Φ means that of T . The pion condensate π decreases as Φ increases and finally vanishes at a critical value Φ_c of Φ . Below Φ_c , the average phase factor is always zero, while π is finite. Above Φ_c , inversely, the average phase factor is finite, while π is always zero. Thus, there is a negative correlation between the average phase factor and the pion condensate. This property is also seen in the NJL model [12]. In contrast, there exists a positive correlation between the average phase factor and the Polyakov loop: the average phase factor is zero at small Φ such as $\Phi < \Phi_c$, but at large Φ such as $\Phi > \Phi_c$ the average phase factor is finite and an increasing function of Φ . In the $\Phi = 1$ limit, the average phase factor

tends to 1. This implies that the NJL model overestimates the average phase factor compared with the PNJL model, since $\Phi = 1$ in the NJL model. This is true, as shown below in Fig. 2.

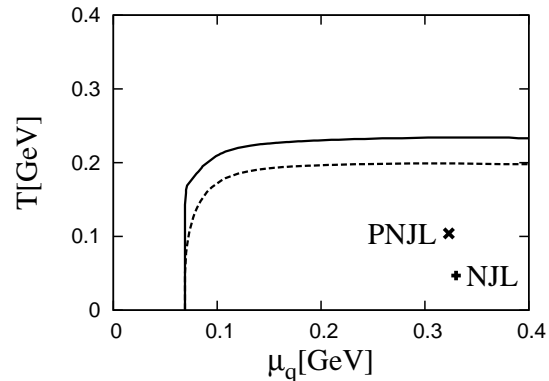


Fig. 2: Boundary of the $\langle e^{2i\theta} \rangle = 0$ region in μ_q - T plane. A solid (dashed) line represents the boundary in the PNJL (NJL) model. Symbols \times and $+$ stand for critical endpoints of the PNJL and NJL models, respectively.

Figure 2 shows a boundary of the region where $\langle e^{2i\theta} \rangle = 0$. The solid (dashed) curve is a result of the PNJL (NJL) model. The region is wider in the PNJL model compared with the NJL model. Thus, the fact that $\Phi < 1$ in the PNJL model makes the region wider and the average phase factor smaller outside the region. The critical endpoint (CEP) of the first-order chiral phase transition is also plotted by a cross (\times) for the PNJL model and a plus ($+$) for the NJL model. For both the models, thus, the CEP and the first-order phase transition are in the $\langle e^{2i\theta} \rangle = 0$ region. This implies that the location of CEP cannot be determined by LQCD directly. The CEP is located at higher T and lower μ_q in the PNJL model compared with the NJL model. However, a relative distance of CEP to the boundary of the $\langle e^{2i\theta} \rangle = 0$ region is almost the same between the two models.

B. Scalar-type eight-quark interaction

The scalar-type eight-quark interaction

$$G_{ss}[(\bar{q}q)^2 + (\bar{q}i\gamma_5\vec{\tau}q)^2]^2 \quad (26)$$

is inevitable to reproduce LQCD data at finite real isospin chemical potential [38] and zero and finite imaginary quark chemical potential [35]. Furthermore, the interaction affects a location of CEP for real μ_q . Therefore, it is important to see how the scalar-type eight-quark interaction affects the average phase factor.

Figure 3 shows μ_q dependence of the average phase factor at $T = 0.9T_c, T_c$ and $1.1T_c$. The solid and dashed lines correspond to the PNJL result with and without the eight-quark interaction. Below T_c such as $T = 0.9T_c$, the scalar-type eight-quark interaction does not affect the average phase factor, and at $T = T_c$ the effect becomes appreciable. Above

T_c such as $T = 1.1T_c$, it enhances the average phase factor sizably.

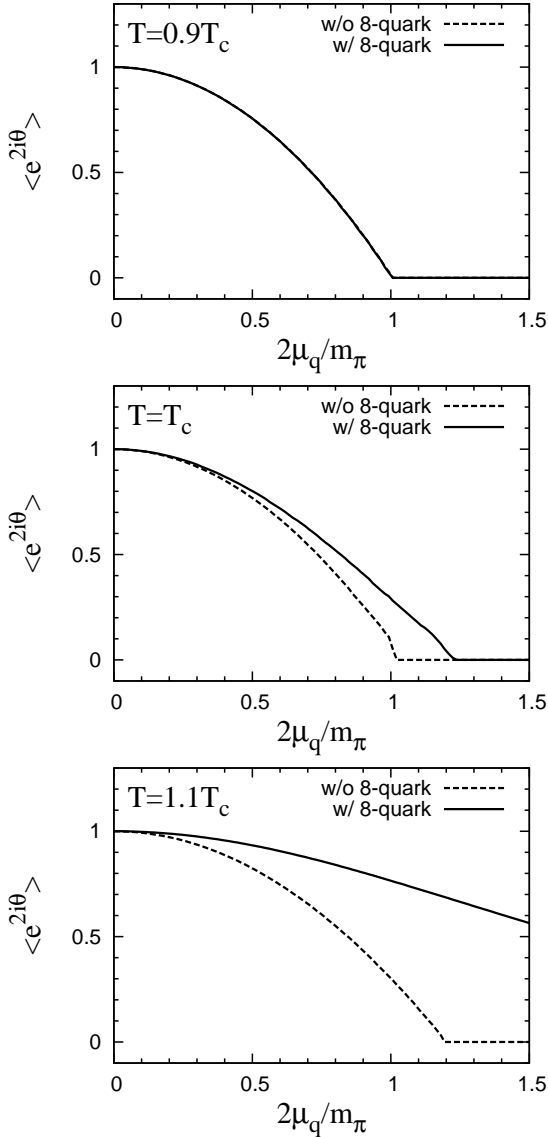


Fig. 3: Effect of scalar-type eight-quark interaction on average phase factor. Solid and dashed lines stand for the PNJL result with and without the eight-quark interaction, respectively.

Figure 4 presents a boundary of the $\langle e^{2i\theta} \rangle = 0$ region and locations of CEP calculated by the PNJL model without and with the scalar-type eight-quark interaction. The eight-quark interaction makes the region smaller. Meanwhile, it shifts the CEP to higher T and lower μ_q . Thus, the relative distance of CEP to the boundary becomes much smaller by the scalar-type eight-quark interaction, although CEP itself lies in the $\langle e^{2i\theta} \rangle = 0$ region even after the scalar-type eight-quark interaction is taken into account. If more accurate LQCD data becomes available in future outside the region $\langle e^{2i\theta} \rangle = 0$, the PNJL model that reproduces the data can predict a location of CEP in principle. The reliability of the prediction may be

proportional to the relative distance. In this sense, the fact that the relative distance is small is important.

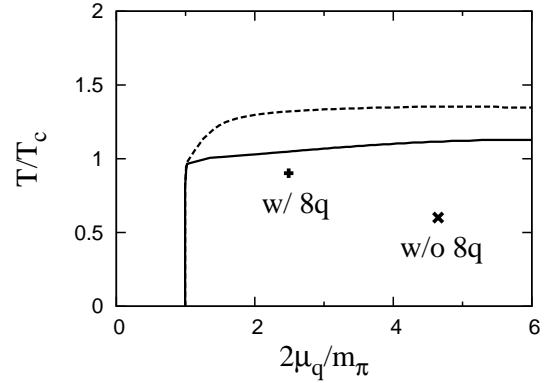


Fig. 4: Effect of the scalar-type 8-quark interaction on locations of CEP and the boundary of the $\langle e^{2i\theta} \rangle = 0$ region. Solid and dashed lines stand for the boundary calculated by the PNJL model with and without the eight-quark interaction, respectively. Symbols + and \times mean the CEP calculated by the PNJL model with and without the eight-quark interaction, respectively.

Figure 5 presents contours of $\langle e^{2i\theta} \rangle$ and Φ in μ_q - T plane calculated by the PNJL model with scalar-type eight-quark interaction. Solid curves correspond to contours of $\langle e^{2i\theta} \rangle = 0, 0.4, \text{ and } 0.8$, while dashed curves do to contours of $\Phi = 0.3, 0.5$ and 0.7 . For $\mu_q < m_\pi/2$, the average phase factor is finite and then calculable with LQCD in principle. For $\mu_q > m_\pi/2$, $\langle e^{2i\theta} \rangle = 0$ at $\Phi \lesssim 0.5$ corresponding to the confinement region. At $\Phi \gtrsim 0.5$ corresponding to the deconfinement region, the factor $\langle e^{2i\theta} \rangle$ is finite and an increasing function of Φ , indicating that there is a positive correlation between $\langle e^{2i\theta} \rangle$ and Φ . Thus, LQCD is feasible only in the deconfinement phase, when $\mu_q > m_\pi/2$.

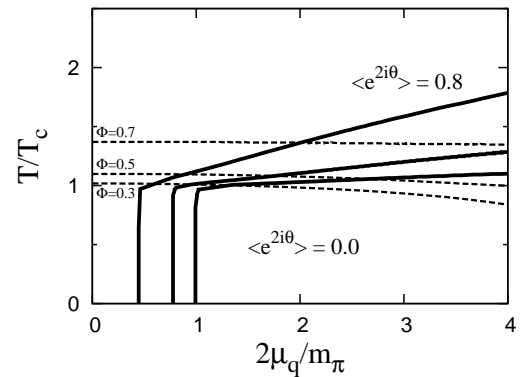


Fig. 5: Contours of the average phase factor and the Polyakov loop in μ_q - T plane. Contours of $\langle e^{2i\theta} \rangle = 0, 0.4, 0.8$ and 1 are drawn by solid curves, while those of $\Phi = 0.3, 0.5$ and 0.7 are by dashed curves.

C. Dynamical mesonic fluctuations

The average phase factor was calculated with LQCD [6] in which the lattice size is $16^3 \times 4$ and the pion mass at vacuum is $m_\pi^{\text{LQCD}} \approx 280$ MeV. In the PNJL calculation, we have then varied the quark mass from $m_0 = 5.5$ MeV to 22.5 MeV to reproduce $m_\pi^{\text{LQCD}} = 280$ MeV. For this value of m_0 , the deconfinement transition temperature becomes a bit higher value, i.e., $T_c = 180$ MeV.

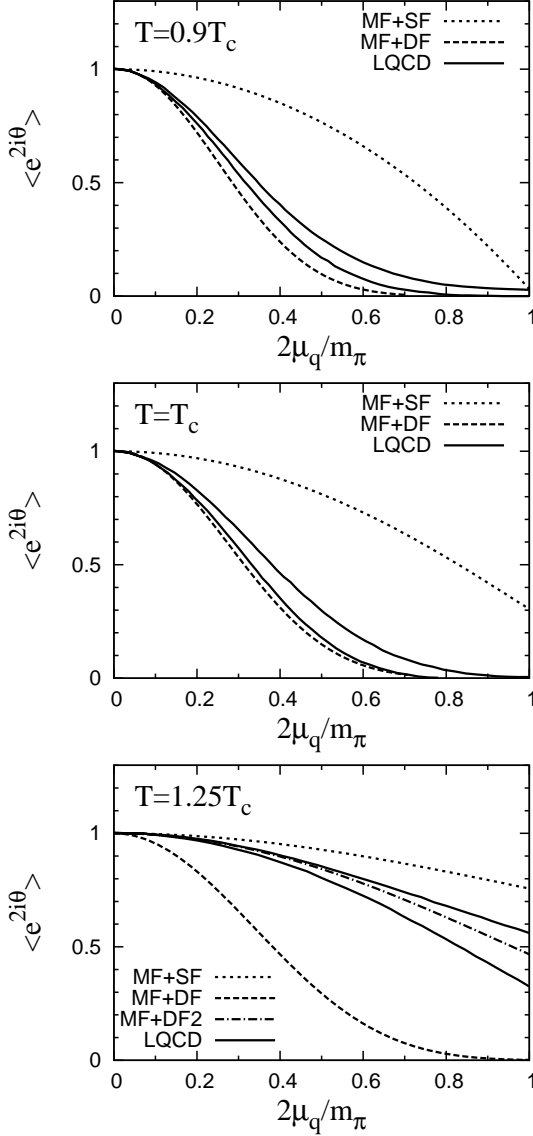


Fig. 6: Effects of mesonic fluctuations on the average phase factor. All the calculations take account of the eight-quark interaction. In MF+DF and MF+DF2 calculations, $m_\pi = m_\pi^{\text{LQCD}}$ and $2.8m_\pi^{\text{LQCD}}$, respectively.

Figure 6 shows μ_q dependence of the average phase factor at $T = 0.9T_c, T_c$ and $1.25T_c$. LQCD result is evaluated from LQCD data at imaginary chemical by assuming a polynomial function. For each panel, the two solid lines delimit

the 90% confidence level region for the extrapolation, while the MF+SF calculation is represented by dotted lines. The MF+SF calculation overestimates LQCD data largely. Therefore, we consider dynamical mesonic fluctuations beyond the MF+SF framework.

Below T_c where the system is confined, it is natural to think that mesonic modes dominate rather than quark modes. Therefore, we should take all possible channels (mesonic modes) in the bubble summation in the random phase approximation (RPA). If there is no pion condensate, σ and π meson modes are decoupled to each other. Hence, the mesonic polarization function matrix does not have off-diagonal elements. Up to order $1/N_c$, where N_c is the number of colors, the thermodynamic potential is obtained by

$$\Omega = \Omega_{\text{MF}} + \Omega_{\text{DF}}, \quad (27)$$

where Ω_{MF} is the mean-field part shown in (16) and Ω_{DF} is the dynamical mesonic fluctuation (DF) part in the ring diagram. Hence, Ω_{DF} is obtained by [44]

$$\Omega_{\text{DF}} = -\frac{i}{2} \int \frac{d^4q}{(2\pi)^4} \ln \det[1 - G_s^* \Pi(q)] \quad (28)$$

with the effective coupling $G_s^* = \text{diag}(G_{s_j}^*)$ for

$$G_{s\sigma}^* = \frac{\partial M}{\partial \sigma}, \quad G_{s\pi_+}^* = G_{s\pi_-}^* = G_{s\pi_0}^* = \frac{\partial N}{\partial \pi}, \quad (29)$$

and the mesonic polarization bubbles

$$\Pi_{jk}(q) = i \int \frac{d^4p}{(2\pi)^4} \text{Tr}[I_j^* \mathcal{S}(p+q) \Gamma_k \mathcal{S}(p)] \quad (30)$$

for $j, k = \sigma, \pi_+, \pi_-, \pi_0$, where Tr is the trace in color, flavor and Dirac indexes and the four momentum integral is defined as $\int d^4q/(2\pi)^4 = iT \sum_n \int d^3\mathbf{q}/(2\pi)^3$ for finite temperature. The meson vertexes Γ_k depend on meson taken; precisely, $\Gamma_\sigma = 1$, $\Gamma_{\pi_+} = i\tau_+\gamma_5$, $\Gamma_{\pi_-} = i\tau_-\gamma_5$, $\Gamma_{\pi_0} = i\tau_3\gamma_5$.

Before calculating dynamical mesonic fluctuations, we clarify a relation between static and dynamical mesonic fluctuations. The effective action of the NJL-type model to $1/N_c$ order is derivable by using the auxiliary field method [17]. The second derivative of the effective action with respect to meson fields yields the inverse meson propagator $G_s^*[1 - G_s^* \Pi(q)]$. Since the static fluctuations are constant, the Hessian matrix (25) is obtained by setting the external momentum $q = 0$ in the inverse propagator:

$$H = G_s^*[1 - G_s^* \Pi(q=0)]. \quad (31)$$

Setting $q = 0$ in (28) reduces Ω_{DF} to $\ln \det[H]$ and the resultant partition function turns out to be (22). Thus, the static mesonic fluctuation $\Omega_{\text{SF}} = \ln \det[H]$ can be regarded as an approximation to the dynamical one Ω_{DF} .

Now we introduce the effective meson mass m_j^* which satisfy

$$\det[1 - G_s^* \Pi(q_0 + \mu_j = m_j^*, \mathbf{q} = \mathbf{0})] = 0 \quad (32)$$

with the meson chemical potentials $\mu_\sigma = \mu_{\pi_0} = 0$, $\mu_{\pi_+} = 2\mu_I$ and $\mu_{\pi_-} = -2\mu_I$. Here note that physical meson masses

are not m_j^* but $m_j = m_j^* - \mu_j$ because they are calculated from q_0 .

Since it is difficult to calculate the dynamical mesonic fluctuations (28) exactly, here we make the pole approximation that neglects the scattering phase shift. If $T < T_c$ and there is no pion condensation, m_j^* is well approximated by the meson mass m_j^0 at vacuum. In this approximation, Ω_{DF} can be obtained by a sum of four quasiparticles, σ , π^+ , π^- and π^0 :

$$\Omega_{\text{DF}} = \sum_j \Omega_j, \quad (33)$$

$$\Omega_j = \int \frac{d^3\mathbf{q}}{(2\pi)^3} \left[\frac{1}{2}(E_j - \mu_j) + T \ln \left(1 - e^{-\beta(E_j - \mu_j)} \right) \right], \quad (34)$$

where $E_j = \sqrt{\mathbf{q}^2 + m_j^{*2}}$. However, corrections due to σ and π^0 mesons are exactly cancelled out between Ω_{1+1} and Ω_{1+1^*} . This framework is referred to as MF+DF in this paper; here, the static fluctuations of ϕ_3 and ϕ_8 are taken into account in the Hessian matrix.

As seen in Fig. 6, at lower T such as $T = 0.9T_c$ and T_c , the MF+DF calculation (dashed line) almost reproduces LQCD data. Above T_c such as $T = 1.25T_c$, the MF+DF calculation underestimates LQCD data. For $T > T_c$, in general, the pion mass becomes larger than m_π^0 [37]. If $m_\pi = 2.8m_\pi^0$ is taken, the calculation (dot-dashed line) is consistent with LQCD data; this calculation is denoted by MF+DF2 in Fig. 6.

IV. SUMMARY

We have calculated the average phase factor of the QCD determinant at finite quark chemical potential μ_q , using the two-flavor version of the PNJL model with the scalar-type eight quark interaction, since the model is successful in reproducing LQCD data not only on the 1+1 system in the limit of no μ_q [35] but also on the 1+1* system with finite isospin chemical potential μ_1 [38]. In the present model, there exists a critical endpoint (CEP) in the 1+1 system with finite μ_q . The CEP lies inside the $\langle e^{2i\theta} \rangle = 0$ region. This implies that the location cannot be determined by LQCD solely.

For $\mu_q > m_\pi/2$, the pion condensate occurs at $\Phi \lesssim 0.5$, so that $\langle e^{2i\theta} \rangle = 0$ there. At $\Phi \gtrsim 0.5$, the factor $\langle e^{2i\theta} \rangle$ is finite and an increasing function of Φ . Thus, there exists a positive correlation between $\langle e^{2i\theta} \rangle$ and Φ . Therefore, LQCD is feasible only in the deconfinement phase with large Φ , when $\mu_q > m_\pi/2$.

The eight-quark interaction makes the $\langle e^{2i\theta} \rangle = 0$ region shrink, while it shifts the CEP toward higher T and smaller μ_q . As a consequence of these properties, a relative distance of the CEP to the boundary of the $\langle e^{2i\theta} \rangle = 0$ region becomes smaller. If more accurate LQCD data becomes available in future outside the $\langle e^{2i\theta} \rangle = 0$ region, we can predict a location of the CEP with the PNJL model the parameters of which are fitted to the data. The accuracy of the model prediction seems to be proportional to the distance. In this sense, the fact that the relative distance is small is important.

For $\mu_q < m_\pi/2$ where no pion condensate takes place, the PNJL calculation with static fluctuations cannot reproduce LQCD data [6] at both $T \leq T_c$ and $T > T_c$. This problem is solved partly by treating dynamical mesonic fluctuations with the pole approximation. The PNJL model with the dynamical mesonic fluctuations reproduces LQCD data at $T \leq T_c$. For $T > T_c$, however, the calculation cannot reproduce the data. The first possible reason is that the meson mass at $T > T_c$ is different from the value at vacuum. The second possible reason is that the pole approximation is not good, because meson at $T > T_c$ is generally in a resonance state. The third possible reason is effects of physical states with nonzero baryon numbers. It is reported in Ref. [6] that the physical states tend to enhance the average phase factor, although the PNJL model does not include such effects. This problem should be solved in future in order to construct a reliable effective model that makes it possible to predict a location of CEP and the phase diagram at finite μ_q .

Acknowledgments

The authors thank K. Kashiwa for useful discussions and suggestions. H. K. also thanks M. Imachi, H. Yoneyama, H. Aoki and M. Tachibana for usefull discussions. Y. S. is supported by JSPS Research Fellow.

-
- [1] J. B. Kogut and D. K. Sinclair Phys. Rev. D **77**, 114503 (2008).
[2] Z. Fodor, and S. D. Katz, Phys. Lett. B **534**, 87 (2002); J. High Energy Phys. **03**, 014 (2002).
[3] C. R. Allton, S. Ejiri, S. J. Hands, O. Kaczmarek, F. Karsch, E. Laermann, Ch. Schmidt, and L. Scorzato, Phys. Rev. D **66**, 074507 (2002); S. Ejiri, C. R. Allton, S. J. Hands, O. Kaczmarek, F. Karsch, E. Laermann, and C. Schmidt, Prog. Theor. Phys. Suppl. **153**, 118 (2004).
[4] P. de Forcrand and O. Philipsen, Nucl. Phys. **B642**, 290 (2002); P. de Forcrand and O. Philipsen, Nucl. Phys. **B673**, 170 (2003).
[5] M. D'Elia and M. P. Lombardo, Phys. Rev. D **67**, 014505 (2003); Phys. Rev. D **70**, 074509 (2004); M. D'Elia, F. D. Renzo, and M. P. Lombardo, Phys. Rev. D **76**, 114509 (2007).
[6] M. D'Elia and F. Sanfilippo, Phys. Rev. D **80**, 014502 (2009).
[7] H. S. Chen and X. Q. Luo, Phys. Rev. **D72**, 034504 (2005); arXiv:hep-lat/0702025 (2007); L. K. Wu, X. Q. Luo, and H. S. Chen, Phys. Rev. **D76**, 034505 (2007).
[8] K. Splittorff and J. J. M. Verbaarschot, Phys. Rev. D **75**, 116003 (2007); K. Splittorff and J. J. M. Verbaarschot, Phys. Rev. D **77**, 014514 (2008).
[9] J. C. R. Bloch and T. Wettig, JHEP **0903**, 100 (2009).
[10] J. Han and M. A. Stephanov, Phys. Rev. D **78**, 054507 (2008).
[11] J. Danzer, C. Gatttringer, C. Liptak, and M. Marinkovic, Phys. Lett. B **682**, 240 (2009).
[12] J. O. Anderson, L. T. Kyllingstad and K. Splittorff, JHEP **1001**, 014 (2010).

- 055 (2010).
- [13] Y. Nambu and G. Jona-Lasinio, Phys. Rev. **122**, 345 (1961); Phys. Rev. **124**, 246 (1961).
- [14] M. Asakawa and K. Yazaki, Nucl. Phys. **A504**, 668 (1989).
- [15] S. P. Klevansky, Rev. Mod. Phys. **64**, 649 (1992).
- [16] T. Hatsuda and T. Kunihiro, Phys. Rep. **247**, 221 (1994).
- [17] T. Sakaguchi, K. Kashiwa, M. Matsuzaki, H. Kouno, and M. Yahiro, Centr. Eur. J. Phys. **6**, 116 (2008).
- [18] K. Kashiwa, H. Kouno, T. Sakaguchi, M. Matsuzaki, and M. Yahiro, Phys. Lett. B **647**, 446 (2007); K. Kashiwa, M. Matsuzaki, H. Kouno, and M. Yahiro, Phys. Lett. B **657**, 143 (2007).
- [19] P. N. Meisinger, and M. C. Ogilvie, Phys. Lett. B **379**, 163 (1996).
- [20] K. Fukushima, Phys. Lett. B **591**, 277 (2004).
- [21] K. Fukushima, Phys. Rev. D **77**, 114028 (2008); Phys. Rev. D **78**, 114019 (2008); Phys. Rev. D **79**, 074015 (2009);
- [22] S. K. Ghosh, T. K. Mukherjee, M. G. Mustafa, and R. Ray, Phys. Rev. D **73**, 114007 (2006).
- [23] E. Megias, E. R. Arriola, and L. L. Salcedo, Phys. Rev. D **74**, 065005 (2006).
- [24] C. Ratti, M. A. Thaler, and W. Weise, Phys. Rev. D **73**, 014019 (2006); C. Ratti, S. Rößner, M. A. Thaler, and W. Weise, Eur. Phys. J. C **49**, 213 (2007).
- [25] S. Rößner, C. Ratti, and W. Weise, Phys. Rev. D **75**, 034007 (2007); S. Rößner, T. Hell, C. Ratti, and W. Weise, Nucl. Phys. **A814**, 118 (2008).
- [26] M. Ciminale, R. Gatto, N. D. Ippolito, G. Nardulli, and M. Ruggieri, Phys. Rev. D **77**, 054023 (2008); M. Ciminale, G. Nardulli, M. Ruggieri, and R. Gatto, Phys. Lett. B **657**, 64 (2007).
- [27] B. -J. Schaefer, J. M. Pawłowski, and J. Wambach, Phys. Rev. D **76**, 074023 (2007).
- [28] Z. Zhang, and Y. -X. Liu, Phys. Rev. C **75**, 064910 (2007).
- [29] S. Mukherjee, M. G. Mustafa, and R. Ray, Phys. Rev. D **75**, 094015 (2007).
- [30] H. Hansen, W. M. Alberico, A. Beraudo, A. Molinari, M. Nardi, and C. Ratti, Phys. Rev. D **75**, 065004 (2007); P. Costa, C. A. de Sousa, M. C. Ruivo, and H. Hansen, Europhys.Lett. **86**, 31001 (2009); P. Costa, M. C. Ruivo, C. A. de Sousa, H. Hansen, and W. M. Alberico, Phys. Rev. D **79**, 116003 (2009); P. Costa, H. Hansen, M. C. Ruivo, and C. A. de Sousa, Phys. Rev. D **81**, 016007 (2010).
- [31] K. Kashiwa, H. Kouno, M. Matsuzaki, and M. Yahiro, Phys. Lett. B **662**, 26 (2008); K. Kashiwa, Y. Sakai, H. Kouno, M. Matsuzaki, and M. Yahiro, J. Phys. G **36**; K. Kashiwa, M. Matsuzaki, H. Kouno, Y. Sakai, and M. Yahiro, Phys. Rev. D **79**, 076008 (2009); H. Kouno, Y. Sakai, K. Kashiwa, and M. Yahiro, J. Phys. G **36**, 115010 (2009).
- [32] W. J. Fu, Z. Zhang, and Y. X. Liu, Phys. Rev. D **77**, 014006 (2008); Phys. Rev. D **79**, 074011 (2009);
- [33] T. Hell, S. Rößner, M. Cristoforetti, and W. Weise, Nucl. Phys. D **79**, 014022 (2009).
- [34] Y. Sakai, K. Kashiwa, H. Kouno, and M. Yahiro, Phys. Rev. D **77**, 051901(R) (2008); Phys. Rev. D **78**, 036001 (2008); Y. Sakai, K. Kashiwa, H. Kouno, M. Matsuzaki, and M. Yahiro, Phys. Rev. D **78**, 076007 (2008).
- [35] Y. Sakai, K. Kashiwa, H. Kouno, and M. Yahiro, Phys. Rev. D **79**, 096001 (2009).
- [36] Y. Sakai, H. Kouno, and M. Yahiro, arXiv: 0908.3088(2009).
- [37] J. Xiong, M. Jin and J. Li, J. Phys. G **36**, 125005 (2009).
- [38] T. Sasaki, Y. Sakai, H. Kouno, and M. Yahiro, arXiv: 0035558 (2010).
- [39] G. Boyd, J. Engels, F. Karsch, E. Laermann, C. Legeland, M. Lütgemeier, and B. Petersson, Nucl. Phys. **B469**, 419 (1996).
- [40] O. Kaczmarek, F. Karsch, P. Petreczky, and F. Zantow, Phys. Lett. B **543**, 41 (2002).
- [41] F. Karsch, Lect. notes Phys. **583**, 209 (2002).
- [42] F. Karsch, E. Laermann, and A. Peikert, Nucl. Phys. B **605**, 579 (2002).
- [43] M. Kaczmarek and F. Zantow, Phys. Rev. D **71**, 114510 (2005).
- [44] P. Zhuang, J. Hüfner, and S. P. Klevansky, Nucl. Phys. A **576**, 525 (1994); C. Mu, and P. Zhuang, Phys. Rev. D **79**, 094006 (2009).

